scientific reports

Check for updates

OPEN

HFD-induced LPS translocation and elevated blood lipids exacerbated the inflammatory response in allergic rhinitis

Shaopeng Peng[1,3], Xuyang Cai[1,3], Jing Tang[1,3], Jinxing Huang[1], Xuefeng Zhao[1], Xingyan Huang[2] & Juan Li[1]✉

Allergic rhinitis (AR) is one of the most prevalent chronic diseases, with studies indicating that a high-fat diet (HFD) may heighten susceptibility to AR. This study aims to investigate the impact of HFD on ovalbumin (OVA)-induced AR using both an OVA-sensitized rat model and a macrophage model treated with palmitic acid (PA). The systemic effects of HFD were explored with respect to intestinal barrier integrity, serum lipids and lipopolysaccharide (LPS) levels, and inflammatory response. In AR rats fed with HFD, there was a reduction in the expression of tight junction proteins in colon tissues, increased serum levels of lipids and LPS, and elevated inflammatory responses in both nasal lavage fluid (NLF) and serum. Additionally, there was enhanced NF-κB and NLRP3 inflammasome activity observed in both nasal and colon tissues. In vitro experiments demonstrated that PA and LPS synergistically amplified inflammatory responses in THP-1-derived macrophages, paralleling the systemic findings. These results suggest that HFD-induced intestinal barrier dysfunction facilitates the translocation of LPS into the bloodstream. Elevated serum LPS level, together with increased blood lipids levels, may exacerbate the inflammatory response in AR through the activation of NF-κB and NLRP3 inflammasome.

Keywords High-fat diet, Allergic rhinitis, OVA, NLRP3 inflammasome, NF-κB

Abbreviations

AR	Allergic rhinitis
HFD	High-fat diet
OVA	Ovalbumin
LPS	Lipopolysaccharide
IFN-γ	Interferon gamma
PA	Palmitic acid
PMA	Phorbol 12-myristate 13-acetate
TC	Total cholesterol
TG	Triglycerides
LDL-C	Low-density lipoprotein cholesterol
HDL-C	High-density lipoprotein cholesterol
NLF	Nasal lavage fluid

Allergic rhinitis (AR), mediated by IgE, is one of the most common chronic disorders. Individuals suffering from AR commonly experience symptoms such as sneezing, and may also have an itchy and runny nose[1]. In recent decades, the annual incidence of AR has been on the rise. Worldwide, it is estimated that 10–40% of the population is affected by AR, with this number exceeding 10 million in China[2]. This has led to a series of societal issues and has become a global health concern. At present, medication is the preferred clinical treatment for AR. However, about 40% of patients are dissatisfied with the efficacy of medication, and some experience adverse drug reactions[3]. Therefore, it is particularly important to minimize triggering factors and focus on the prevention of AR.

[1]Department of Pharmacy, The First Affiliated Hospital of Chongqing Medical University, Chongqing 400016, China. [2]Department of Pharmacy, The People's Hospital of Kaizhou District, Chongqing 405400, China. [3]Shaopeng Peng, Xuyang Cai and Jing Tang contributed equally to this work. ✉email: zpfirst@sina.com

In 2018, Yuan, Y. et al.[4] found that high-fat diet (HFD) has been closely linked to the onset and progression of various diseases, including colitis and allergic airway conditions. Researches have indicated that a dietary pattern rich in high-fat foods may increase susceptibility to AR, with studies identifying a significant positive correlation between margarine intake and the prevalence of AR[5,6]. Additionally, children who consume a high-protein, HFD appear to be at an increased risk of developing AR[7]. Given these findings, dietary control emerges as a promising approach not only for preventing AR but also for mitigating its impact. By reducing exposure to triggering factors through careful dietary management, it may be possible to lessen the burden of AR on affected individuals.

Currently, there are many reports regarding the correlation between HFD and asthma. Research indicates that long-term consumption of a HFD can exacerbate the inflammatory response in mouse models of asthma induced by OVA[8]. Study has shown that HFD activated NLRP3 inflammasome and upregulated TLR4-NF-κB-related protein expression in the lungs of obese asthmatic mice[9], contributing to enhanced inflammation. Specifically, Jeong et al.[10] found that HFD-fed mice exhibited increased expression of the NLRP3 inflammasome, which worsened asthma progression. Furthermore, Hur et al.[11] reported that the activation of NLRP3 inflammasome by HFD in obese asthmatic mice was associated with increased IL-1β expression, highlighting a mechanistic link between dietary fat intake and asthma severity.

However, the mechanisms by which HFD regulated AR remains unclear. Otolaryngologists worldwide agree with the concept of "one airway, one disease", suggesting a close connection between the upper and lower respiratory tracts, and recognizing that diseases in these areas were closely related[12,13]. Given the shared pathogenic mechanisms between allergic rhinitis and asthma, we speculate that HFD may also influence the inflammatory state of AR in a similar manner to its impact on asthma.

Therefore, this study aims to investigate the effect of HFD on the inflammatory response associated with AR through both in vivo and in vitro experiments, and seeks to clarify whether the activation of NF-κB and NLRP3 inflammasome plays a role in the mechanism by which HFD exacerbates AR.

Results

Effects of HFD on the general conditions of AR rats

Effects of HFD on nasal symptom scores and body weight in AR rats

Following the protocols from previous studies[14–16], we successfully established a rat model of AR induced by OVA in combination with HFD (Fig. 1A). It was observed that the rats with HFD gained more weight than those in the normal diet groups (Fig. 1B). As shown in Fig. 1C, the nasal symptom score in the OVA-sensitized normal diet group (S + ND) increased more than two folds compared to the normal diet control group (ND) ($P < 0.0001$ vs. ND group). Moreover, rats in the S + HFD group exhibited more severe AR symptoms than those in the S + ND group ($P < 0.05$ vs. S + ND group).

Effects of HFD on inflammatory indicators and OVA-specific IgE in NLF of AR rats

The levels of IL-4, IL-6, IL-13, IL-1β and OVA-specific IgE in NLF of S + ND group were significantly elevated compared to those in ND group ($P < 0.05$, $P < 0.001$, $P < 0.05$, $P < 0.01$, $P < 0.01$ vs. ND group, respectively) (Fig. 1D and E). The levels of IL-4, IL-5, IL-6, TNF-α, IL-1β and OVA-specific IgE in NLF of S + HFD group were obviously higher than those in S + ND group ($P < 0.05$ for IL-4, IL-6, TNF-α and IL-1β; $P < 0.0001$ for IL-5; $P < 0.01$ for OVA-specific IgE vs. S + ND group) (Fig. 1D and E).

Effects of HFD on histopathology of nasal mucosa in AR rats

Eosinophilic infiltration, mast cell accumulation, a reduction in cilia cells, as well as vasodilation were present in the nasal mucosa of rats in the S + HFD and S + ND groups, with a more pronounced manifestation observed in the S + HFD group. The ND and HFD groups of rats exhibited minimal inflammatory cell presence and maintained a more normotypic mucosal structure (Fig. 1F and G).

Effects of HFD on histopathology and intestinal epithelial tight junctions in the colon of AR rats

In S + HFD group, colon tissues exhibited reduced wall thickness, irregular glandular morphology, and evidence of inflammatory infiltration (Fig. 2A). In HFD group, colon tissues showed moderate colonic crypt degeneration along with inflammatory cell infiltration, whereas the S + ND group displayed localized inflammatory cell infiltration in the colon tissues (Fig. 2A).

Immunohistochemical analysis demonstrated weak staining of ZO-1 and Occludin in the colon tissues of HFD and S + HFD groups, whereas these tight junction proteins were highly expressed in the colon tissues of ND and S + ND groups (Fig. 2B and C).

Effects of HFD on the serum levels of lipids, LPS, inflammatory indicators and OVA-specific IgE in AR rats

We assessed the serum lipid parameters in all groups and found that HFD significantly increased the serum levels of TG, TC, and LDL-C, while decreasing the serum level of HDL-C (Fig. 3A). Additionally, it was found that the serum LPS levels were elevated in rats with HFD, both in the HFD group and the sensitized plus HFD group (S + HFD) (Fig. 3B).

Furthermore, the serum levels of IL-6, TNF-α, IL-1β and OVA-specific IgE in the S + ND group were significantly higher than those in the ND group (all $P < 0.05$ vs. ND group) (Fig. 3C and D). The serum levels of IL-4, IL-6, IL-13, TNF-α, IL-1β and OVA-specific IgE in the S + HFD group were obviously higher than those in the S + ND group ($P < 0.05$ for IL-4, TNF-α, IL-1β and OVA-specific IgE; $P < 0.01$ for IL-6; $P < 0.0001$ for IL-13 vs. S + ND group) (Fig. 3C and D).

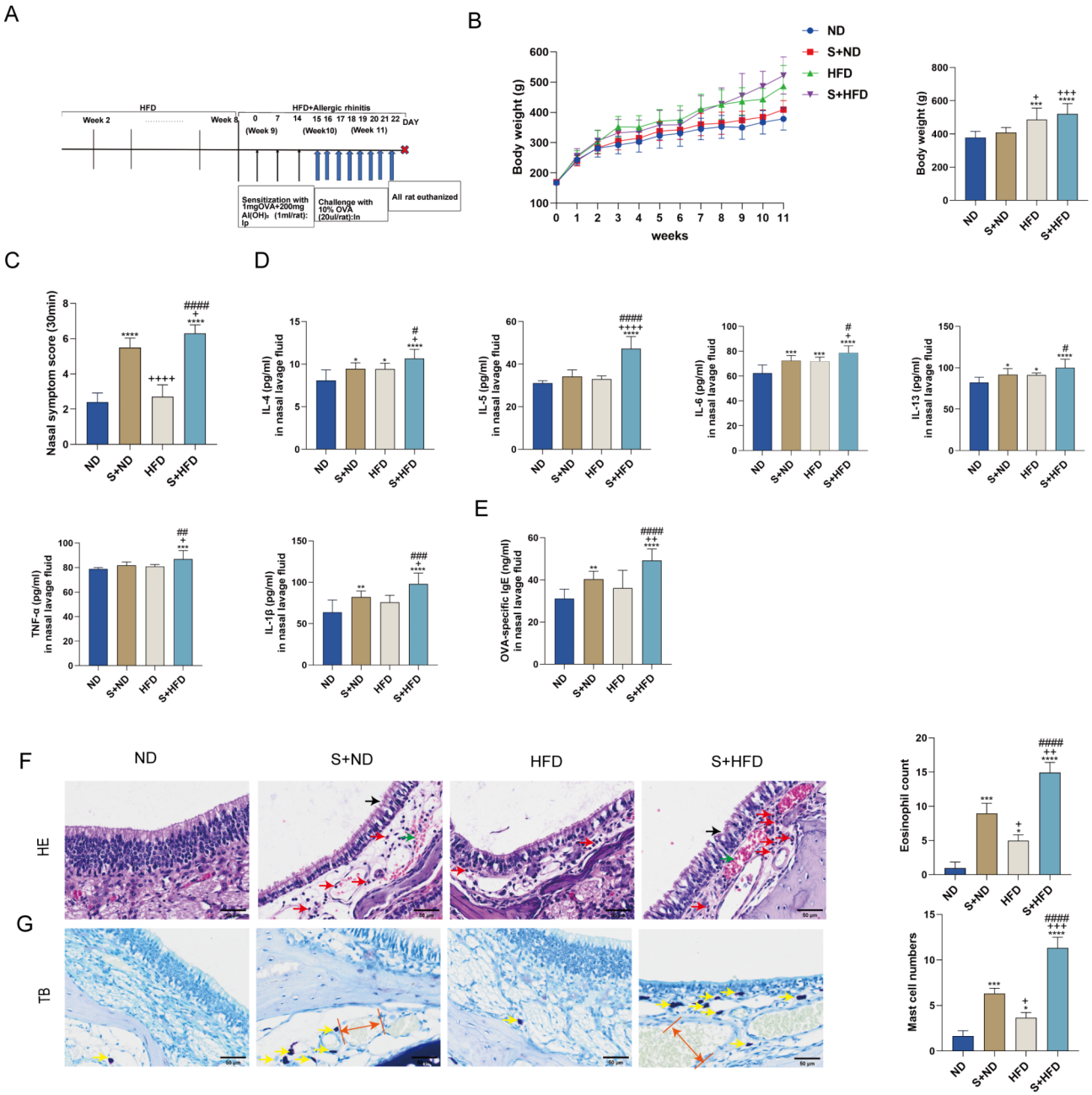

Fig. 1. Effects of HFD on the general conditions of AR rats. (**A**) Diet and sensitization experimental protocol: rats were fed a HFD or a ND for 11 weeks, and OVA sensitization was performed for 3 weeks starting from the 9th week. The weight of the rats was recorded weekly. (**B**) Body weight statistics of rats over the 11-week period and the body weight chart for week 11. (**C**) Statistical chart of nasal symptom scores in rats. (**D**) IL-4, IL-5, IL-6, IL-13, TNF-α, and IL-1β levels in the NLF from all study groups. (**E**) OVA-specific IgE levels in the NLF from all study groups. (**F** and **G**) Histological analysis of nasal tissue sections stained with H&E and TB (scale bar = 50 μm). Red arrows indicate eosinophils, with significant eosinophil aggregation seen in the S + ND and S + HFD groups, interpreted as eosinophilic infiltration. Yellow arrows point to mast cells, which are increased in the S + ND and S + HFD groups. Black arrows point to ciliated cells, with notable ciliated cell loss in the S + ND and S + HFD groups. Green arrows indicate blood cells, while orange double-headed arrows represent vasodilation. Values are represented as mean ± SD. ND: normal diet control group; S + ND: OVA-sensitized with normal diet group; HFD: high-fat diet control group; S + HFD: OVA-sensitized with high-fat diet group ($n = 10$ in each group). $^{*}P < 0.05$, $^{**}P < 0.01$, $^{***}P < 0.001$ and $^{****}P < 0.0001$ compared to the ND group; $^{+}P < 0.05$, $^{++}P < 0.01$, $^{+++}P < 0.001$ and $^{++++}P < 0.0001$ compared to the S + ND group; $^{\#}P < 0.05$, $^{\#\#}P < 0.01$, $^{\#\#\#}P < 0.001$ and $^{\#\#\#\#}P < 0.0001$ compared to the HFD group.

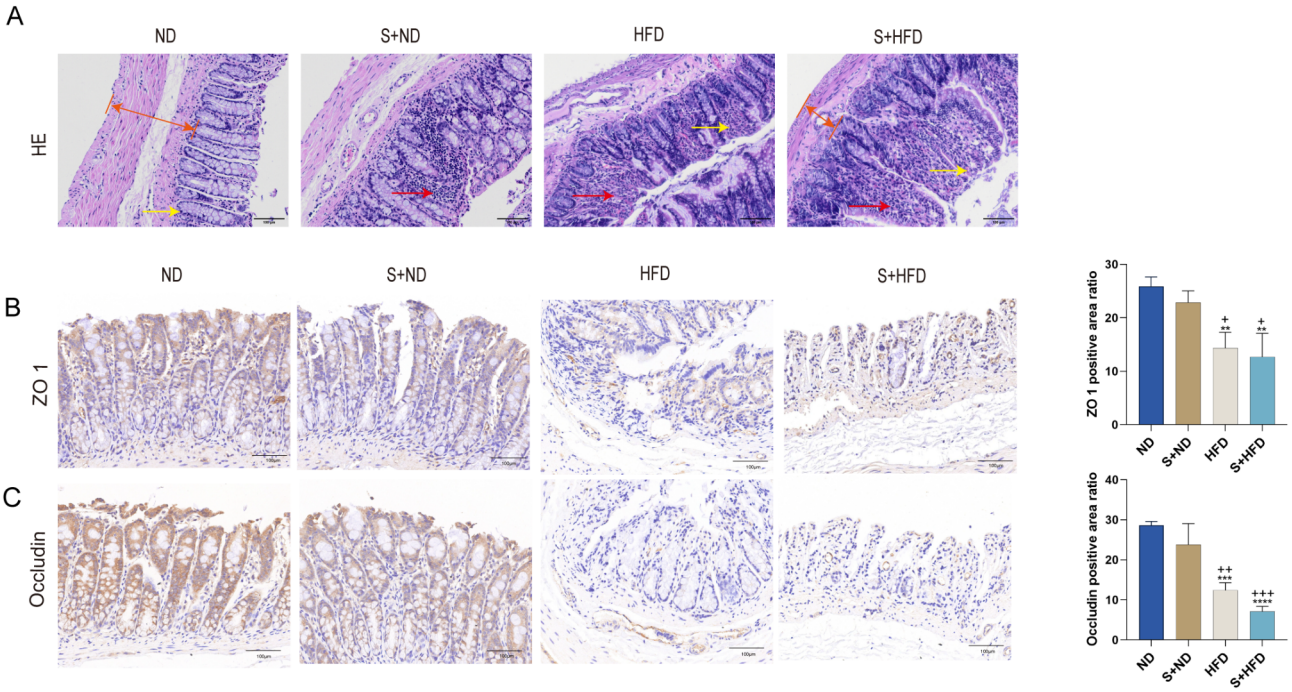

Fig. 2. Effects of HFD on histopathology and intestinal epithelial tight junctions in the colon of AR rats. (**A**) Images of rat colon tissues stained with H&E (scale bar = 100 μm). Red arrows indicate inflammatory cell infiltration. Yellow arrows point to glandular morphology and orange double-headed arrows represent the intestinal wall thickness from the crypt to the serosa. Immunohistochemical staining of ZO-1 (**B**) and occludin (**C**) in the colon of rats (scale bar = 100 μm). The percentage area (%Area) of each image was quantified using ImageJ.lnk software, and subsequently analyzed statistically using GraphPad Prism software. $^{*}P < 0.05$, $^{**}P < 0.01$, $^{***}P < 0.001$ and $^{****}P < 0.0001$ compared to the ND group; $^{+}P < 0.05$, $^{++}P < 0.01$, $^{+++}P < 0.001$ and $^{++++}P < 0.0001$ compared to the S + ND group; $^{\#}P < 0.05$, $^{\#\#}P < 0.01$, $^{\#\#\#}P < 0.001$ and $^{\#\#\#\#}P < 0.0001$ compared to the HFD group, $n = 3$ in each group.

Effects of HFD on the expression of NF-κB and NLRP3 inflammasome in the nasal mucosa of AR rats

Immunohistochemical analysis showed that there was a barely expression of NLRP3 and NF-κB p65 in the nasal mucosa of ND group, whereas NLRP3 and NF-κB p65 were highly expressed in the nasal mucosa of OVA-sensitized groups (S + HFD and S + ND). Notably, the highest expression was found in the nasal mucosa of S + HFD group (Fig. 4A, B). In HFD group, weak staining for NLRP3 and NF-κB p65 was observed in the nasal mucosa (Fig. 4A, B).

The above results were further confirmed by Western blot and RT-PCR (Fig. 4C, D). In the nasal mucosa, both the S + HFD and S + ND groups exhibited significantly higher protein levels of NLRP3 inflammasome components (NLRP3, Caspase-1, ASC) compared to their respective control groups (ND for S + ND, and S + ND for S + HFD). Moreover, the S + HFD group showed markedly increased mRNA levels of these NLRP3 inflammasome components compared to the S + ND group. Both S + HFD and S + ND groups also showed an elevated mRNA expression of NF-κB p65 and increased protein expression of Cleaved-Caspase-1 compared to their respective controls. Additionally, the relative expression of phosphorylated NF-κB p65 to total NF-κB p65 was also increased in both S + HFD and S + ND groups compared to their respective controls. Notably, these effects were more pronounced in the S + HFD group compared to the S + ND group.

Effects of HFD on the expression of NF-κB and NLRP3 inflammasome in the colon of AR rats

Immunofluorescence analysis showed that the fluorescence intensity of NF-κB p65, NLRP3, and Caspase-1 in the colon tissues of rats from the S + HFD group was higher than those in the S + ND group (Fig. 5A–C).

Compared to the S + ND group, Western blot and RT-PCR analyses showed that the S + HFD group had significantly elevated levels of NLRP3, Caspase-1, and ASC proteins and mRNAs, NF-κB p65 mRNA, and Cleaved-Caspase-1 protein in the colon tissues. Moreover, the relative protein expression of phosphorylated NF-κB p65 to total NF-κB p65 in the colon tissues was obviously increased in S + HFD group than those in S + ND group. (Fig. 5D–E).

Effects of PA and LPS on the inflammation of macrophage

The THP-1 cell line was induced to differentiate into macrophage using PMA to validate the findings from in vivo experiments. As shown in Fig. 6A, neither 100 μM PA nor the IFN-γ + LPS treatment affected macrophage viability. Oil Red O staining demonstrated a significant accumulation of lipid droplets in the PA + LPS and

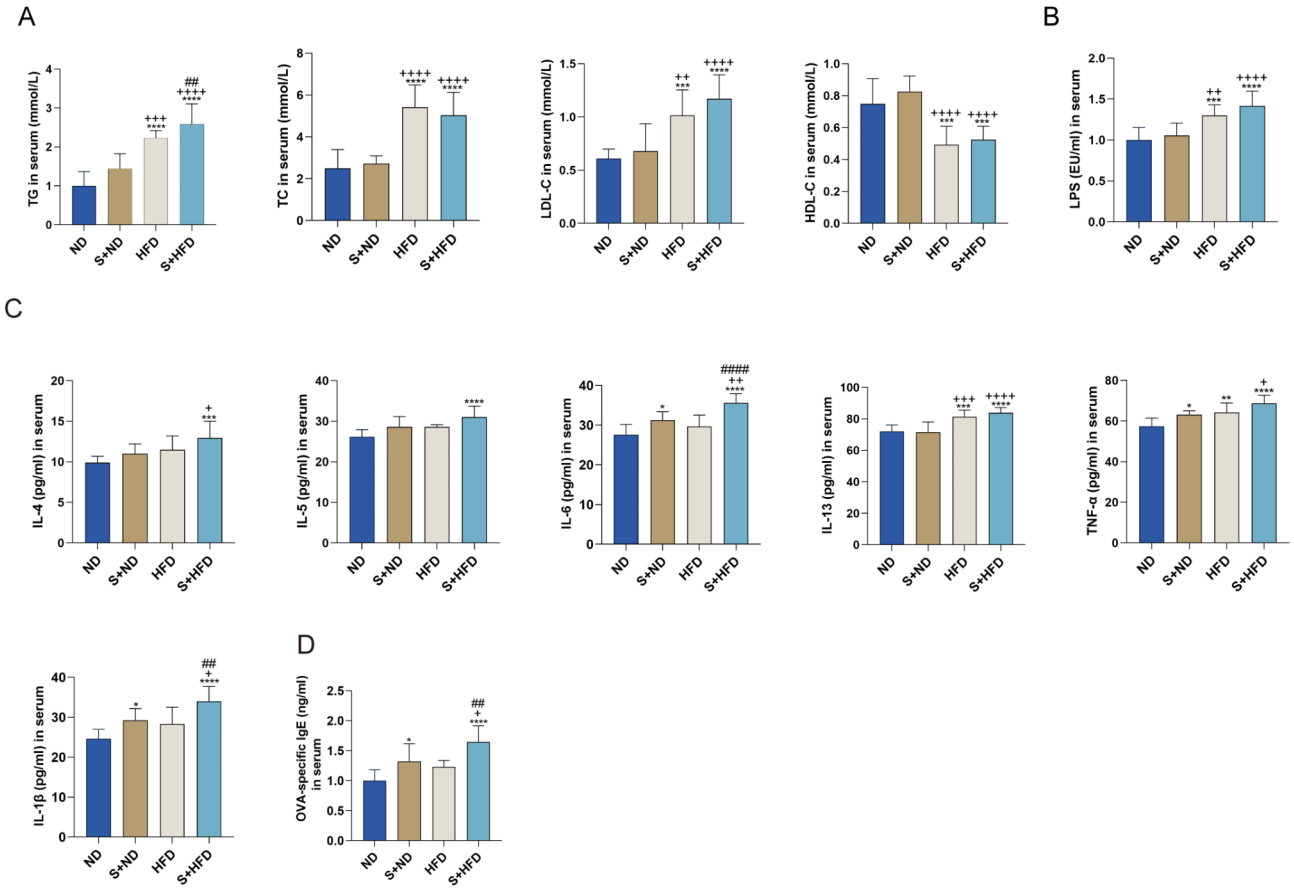

Fig. 3. Effects of HFD on the serum levels of lipids, LPS, inflammatory indicators and OVA-specific IgE in AR rats. (**A**) Serum levels of total cholesterol (TC), triglyceride (TG), low-density lipoprotein cholesterol (LDL-C) and high-density lipoprotein cholesterol (HDL-C) in all study groups. (**B**) Serum LPS levels from all study groups. (**C**) Serum levels of IL-4, IL-5, IL-6, IL-13, TNF-α, and IL-1β from all study groups. (**D**) Serum OVA-specific IgE levels from all study groups. $^{*}P<0.05$, $^{**}P<0.01$, $^{***}P<0.001$ and $^{****}P<0.0001$ compared to the ND group; $^{+}P<0.05$, $^{++}P<0.01$, $^{+++}P<0.001$ and $^{++++}P<0.0001$ compared to the S + ND group; $^{\#}P<0.05$, $^{\#\#}P<0.01$, $^{\#\#\#}P<0.001$ and $^{\#\#\#\#}P<0.0001$ compared to the HFD group, $n=10$ in each group.

PA groups compared to the control and LPS-only groups (Fig. 6B). Compared to PA or LPS alone, PA + LPS significantly increased NLRP3 and Caspase-1 protein and mRNA levels, NF-κB p65 mRNA levels, and Cleaved-Caspase-1 protein levels in THP-1-derived macrophages (Fig. 6C, D). Additionally, this combination elevated the relative expression of phosphorylated NF-κB p65 to total NF-κB p65 (Fig. 6C, D).

Discussion

In this study, we investigated the effect of HFD on AR and its underlying mechanism. Our results demonstrated that in OVA-sensitized rats, HFD exacerbated nasal symptoms, and increased inflammatory cell infiltration while promoting mast cell degranulation within the nasal mucosa. Furthermore, HFD led to increased inflammatory cell infiltration in colon tissues, decreased expression of intestinal tight junction proteins, elevated serum levels of lipids and LPS, and heightened inflammatory responses in both NLF and serum. Additionally, HFD significantly upregulated the expressions of NLRP3, Caspase-1, ASC, and NF-κB in both nasal mucosa and colon tissues of OVA-sensitized AR rats. In vitro experiments demonstrated that the combination of LPS and PA resulted in a significant increase in the expression of NLRP3, Caspase-1, and NF-κB compared to PA or LPS alone.

According to the literature[17], HFD could induce intestinal barrier damage and increased permeability in rats by downregulating tight junction proteins such as occludin and ZO-1. This dietary pattern also led to elevated levels of LPS, a common microbial metabolite, within the intestinal tract[18]. LPS further compromised the integrity of the intestinal barrier by reducing the expression of ZO-1, occludin, and claudin-1[19], thereby increasing intestinal permeability. The heightened permeability allowed LPS to translocate from the intestinal tract into the bloodstream, significantly elevating serum LPS levels in obese individuals[20]. Consistent with these studies, our results demonstrated that in rats fed with HFD, the expression of the intestinal tight junction proteins occludin and ZO-1 was reduced in colonic tissues, while serum LPS levels were elevated. These findings suggest that HFD compromises the intestinal barrier, leading to the translocation of LPS into the bloodstream.

Elevated serum LPS is recognized as a stimulatory factor that promotes systemic inflammation and contributes to the progression of several chronic inflammatory diseases[21]. It also serves as a stimulus for nasal

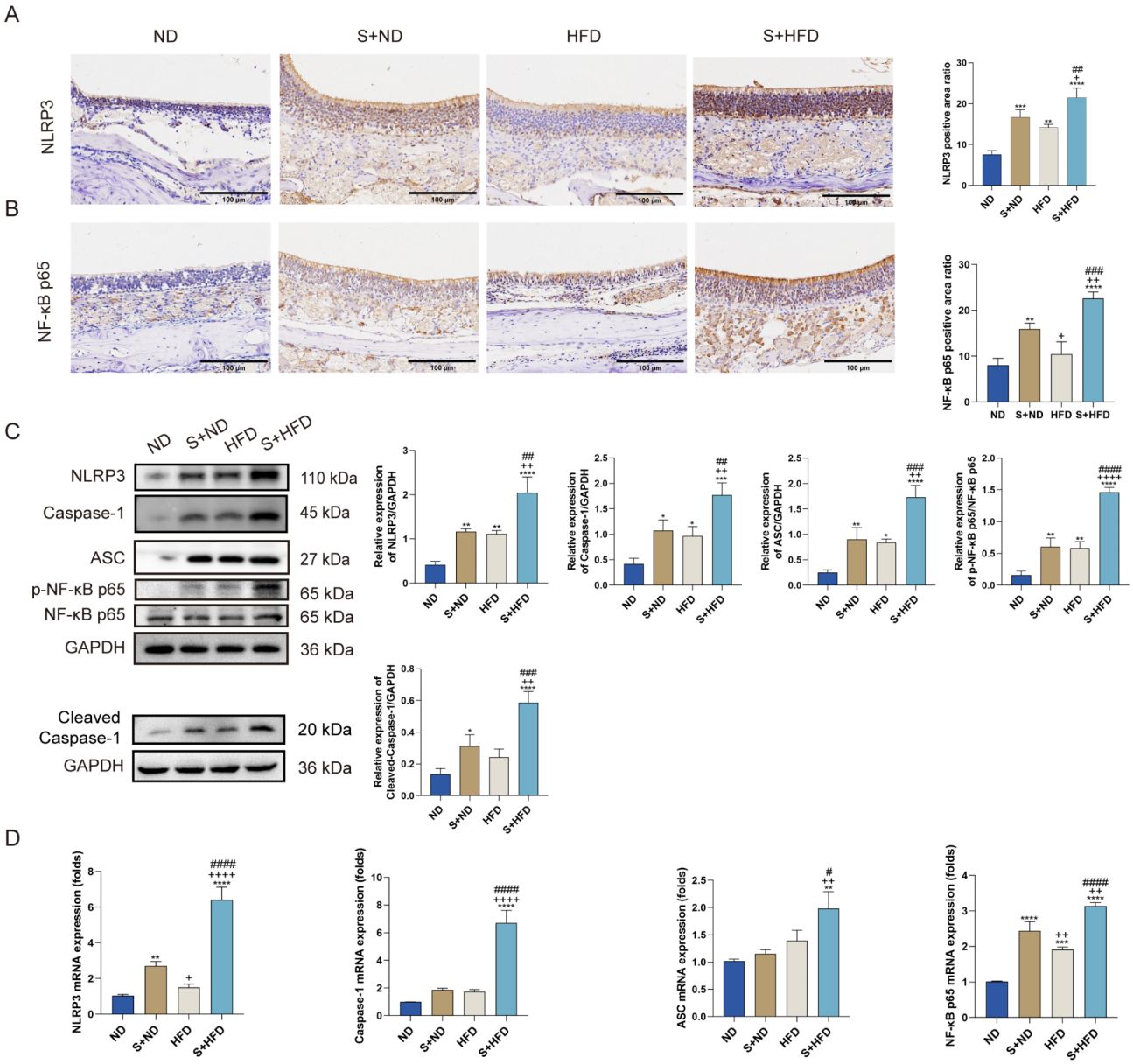

Fig. 4. Effects of HFD on the expression of NF-κB and NLRP3 inflammasome in the nasal mucosa of AR rats. Immunohistochemical staining of NLRP3 (**A**) and NF-κB p65 (**B**) in the nasal mucosa of rats (scale bar = 100 μm), the percentage area (%Area) of each image was quantified using ImageJ.lnk software and subsequently analyzed statistically using GraphPad Prism software. (**C**) Relative protein expression of NLRP3, Caspase-1, ASC, p-NF-κB p65, NF-κB p65, and Cleaved-Caspase-1 in the nasal mucosa of rats. Original blots/gels are presented in Supplementary Fig. S1. (**D**) Relative mRNA expression of NLRP3, Caspase-1, ASC, and NF-κB p65 in the nasal mucosa of rats, values are presented as mean ± SD ($n = 3$ in each group). $^{*}P < 0.05$, $^{**}P < 0.01$, $^{***}P < 0.001$ and $^{****}P < 0.0001$ compared to the ND group; $^{+}P < 0.05$, $^{++}P < 0.01$, $^{+++}P < 0.001$ and $^{++++}P < 0.0001$ compared to the S + ND group; $^{\#}P < 0.05$, $^{\#\#}P < 0.01$, $^{\#\#\#}P < 0.001$ and $^{\#\#\#\#}P < 0.0001$ compared to the HFD group.

inflammation. Hara et al.[22] reported that intranasal instillation of LPS can induce nasal inflammation in mice. Zhang et al.[23] reported that LPS stimulation of the nasal mucosa could activate NF-κB in mucosal epithelial cells and local inflammatory cells, leading to the release of Th cytokine, which played an immunoregulatory role in the onset and development of allergic diseases. Ding et al. stimulated human nasal epithelial cells with LPS and adenosine triphosphate (ATP), and the results showed that LPS/ATP could upregulate the expression levels of NLRP3, Caspase-1 p10/p20, ASC, GSDMD-N, and IL-1β, inducing cell pyroptosis and exacerbating nasal inflammatory response[24]. Moreover, Bai et al.[25] found that OVA could induce changes in gut microbiota, damage to intestinal mechanical barrier, and inflammatory responses driven by NLRP3 inflammasome in AR mice. And several studies have implicated that NLRP3 inflammasome and NF-κB were involved in the pathogenesis of AR[26–28]. In our study, we found that HFD increased the expression of NLRP3, Caspase-1, ASC,

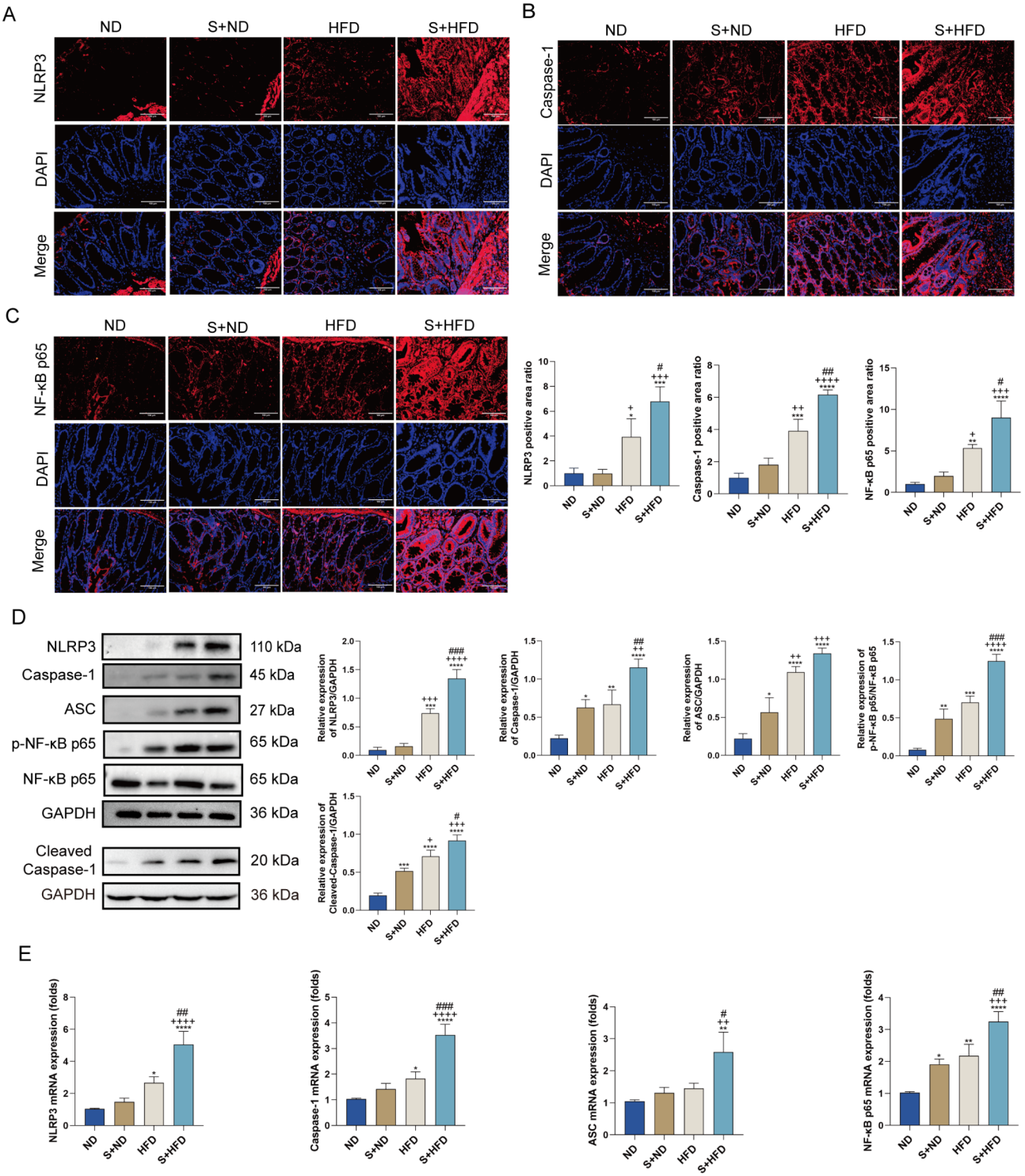

Fig. 5. Effects of HFD on the expression of NF-κB and NLRP3 inflammasome in the colon of AR rats. Immunofluorescence images of the expression of NLRP3 (**A**), Caspase-1 (**B**) and NF-κB p65 (**C**) in the colon of rats (scale bar = 100 μm). (**D**) Relative protein expression levels of NLRP3, Caspase-1, ASC, p-NF-κB p65, NF-κB p65, and Cleaved-Caspase-1 in the colon of rats. Original blots/gels are presented in Supplementary Fig. S1. (**E**) Relative mRNA expression levels of NLRP3, Caspase-1, ASC and NF-κB p65 in the colon of rats. Values are represented as mean ± SD ($n = 3$ in each group). $^{*}P < 0.05$, $^{**}P < 0.01$, $^{***}P < 0.001$ and $^{****}P < 0.0001$ compared to the ND group; $^{+}P < 0.05$, $^{++}P < 0.01$, $^{+++}P < 0.001$ and $^{++++}P < 0.0001$ compared to the S + ND group; $^{\#}P < 0.05$, $^{\#\#}P < 0.01$, $^{\#\#\#}P < 0.001$ and $^{\#\#\#\#}P < 0.0001$ compared to the HFD group.

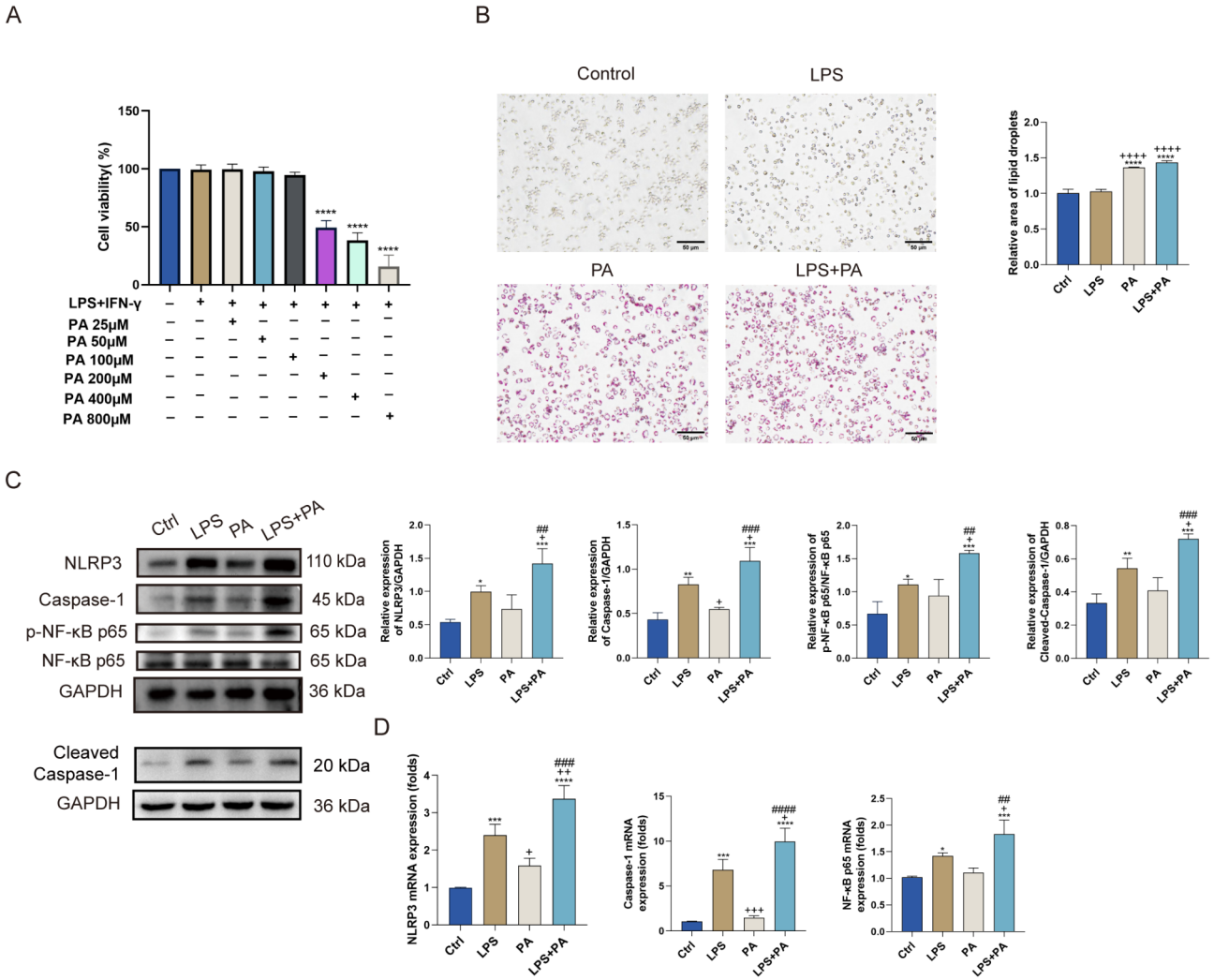

Fig. 6. Effects of PA and LPS on the inflammation of macrophage. (**A**) Cytotoxic effects of PA (25–800 μM) on THP-1 cells during LPS + IFN - γ treatment for 24 h. (**B**) Oil red O staining images of macrophages differentiated from the THP-1 cell line (scale bar = 50 μm). (**C**) Relative protein expression levels of NLRP3, Caspase-1, p-NF-κB p65, NF-κB p65 and Cleaved-Caspase-1 in macrophages differentiated from the THP-1 cells line. Original blots/gels are provided in Supplementary Fig. S1. (**D**) Relative mRNA expression levels of NLRP3, Caspase-1, and NF-κB p65 in macrophages differentiated from the THP-1 cell line, values are presented as mean ± SD ($n = 3$ in each group). $^{*}P < 0.05$, $^{**}P < 0.01$, $^{***}P < 0.001$ and $^{****}P < 0.0001$ compared to the Ctrl group; $^{+}P < 0.05$, $^{++}P < 0.01$, $^{+++}P < 0.001$ and $^{++++}P < 0.0001$ compared to the LPS group; $^{\#}P < 0.05$, $^{\#\#}P < 0.01$, $^{\#\#\#}P < 0.001$ and $^{\#\#\#\#}P < 0.0001$ compared to the PA group.

and NF-κB in the nasal mucosa and colon of AR rats, thereby exacerbating the inflammatory response in these tissues. Additionally, HFD significantly elevated the serum LPS levels. These results, combined with findings from the literature, suggest that the NLRP3 inflammasome and NF-κB may be involved in the exacerbation of inflammation induced by HFD in AR, and are associated with elevated levels of LPS.

Palmitic acid (PA), the predominant saturated free fatty acid in the body, accounts for 30-40% of the total plasma free fatty acids and has been shown to elicit inflammatory responses[29]. Wen et al. reported that PA acted as a second signal for NLRP3 inflammasome activation, facilitating the processing of IL-1β and IL-18, and promoting the NF-κB activation, which enhanced the transcription of other pro-inflammatory cytokines[30]. THP-1 cells, derived from an acute monocytic leukemia patient, served as a human monocytic cell line widely used as an in vitro macrophage inflammation model due to their ability to differentiate into macrophages when stimulated by PMA. Bai et al.[25] established an in vitro AR inflammation model using THP-1 cells differentiated into macrophages stimulated with LPS + IFN-γ, demonstrating that this combination can induce an inflammatory response. Moreover, Arqom et al. demonstrated that PA can amplify the pro-inflammatory effects of LPS in THP-1 cells[31]. Yang et al.[9] found that the combination of LPS and PA led to an increased expression of inflammation-related proteins, including NLRP3, ASC, Caspase-1, TLR4, and p-p65, in THP-1 cells compared to the treatment with LPS or PA alone. Additionally, it has been reported that HFD-induced obesity triggered a low-grade systemic inflammatory response, similar to that observed following treatment

with LPS and PA[29]. Our results demonstrated that the combination of PA and LPS significantly enhanced the activation of the NLRP3 inflammasome and upregulated the expression of NF-κB compared to LPS alone. These findings are consistent with our in vivo experimental results and the aforementioned studies, suggesting that lipids can significantly enhance the pro-inflammatory effects of LPS. This potentiation may occur through the activation of the NLRP3 inflammasome and related inflammatory pathways, as well as by upregulating the expression of associated factors.

In this study, we identified a potential mechanism by which HFD exacerbated AR. Our findings suggest that HFD-induced LPS translocation, together with elevated blood lipid levels, significantly intensifies the inflammatory response in AR. This effect appears to involve the activation of NLRP3 inflammasome and NF-κB. Moreover, further studies may be required to investigate additional potential inflammatory pathways and to explore the relationship between gut microbes, NLRP3 inhibitors, *Nlrp3*$^{-/-}$ animals or cells and AR. Additionally, it is necessary to explore potential therapeutic interventions. Altogether, reducing high-calorie and high-fat food intake may aid in reducing susceptibility to AR and provide new prevention and treatment strategies for AR in clinical practice.

Conclusion

HFD-induced LPS translocation, together with elevated blood lipids, may exacerbate the inflammatory response in AR via the NLRP3 inflammasome and NF-κB.

Materials and methods

Animals

The present study was performed on 40 specific pathogen-free (SPF) Wistar rats, weighing approximately 160 g and aged 6 to 8 weeks, with an equal distribution of males and females. The rats were obtained from Beijing Vital River Laboratory Animal Technology Company (License No: SCKY (Jing) 2021-0006). They were housed in a controlled environment maintained at 22 ± 2 ℃ with a 12:12 h light–dark cycle. During the acclimation and experimental periods, the animals had free access to food and water. The protocol was reported in accordance with ARRIVE guidelines (https://arriveguidelines.org). The animal experiment was approved by the Animal Experiment Ethics Committee of Chongqing Medical University (Approval number: IACUC-CQMU-2024-0436).

Animal grouping and modeling

Animals were randomly divided into four groups (10 rats per group, 5 males and 5 females): normal diet control group (ND), ovalbumin (OVA)-sensitized with normal diet group (S + ND), high-fat diet control group (HFD), and OVA-sensitized with high-fat diet group (S + HFD). The modeling protocol was adapted from the previous literature[14,15]. To further investigate the effects of HFD on AR rats, we selected a diet plan with higher fat content (60% of energy from fat)[16]. Briefly, animals in the high-fat diet groups (HFD and S + HFD) were fed a high-fat diet (60% of energy from fat, D12492), while those in the normal diet groups (ND and S + ND) received standard rat chow (10% of energy from fat, D12450B). All rats were maintained on their respective diets for 8 weeks. Beginning in the ninth week, rats in S + ND and S + HFD groups were sensitized with OVA according to the following protocol. Rats in the sensitized groups received intraperitoneal injections of 1 mg OVA (A5503; Sigma-Aldrich, St. Louis, USA) and 200 mg alum hydroxide gel (239186; Sigma-Aldrich, St. Louis, USA) dissolved in 0.9% saline on days 0, 7 and 14[14]. From day 15, these rats were challenged by nasal administration of 10% OVA (physiological saline as the solvent, 10 ul per nostril) once daily for seven consecutive days[15]. Meanwhile, rats in the ND and HFD groups received nasal drops of physiological saline. The experiment lasted for 11 weeks, during which the body weights of the rats were recorded weekly.

Evaluation of nasal symptoms

Following the final challenge on day 22, rats were resettled in breeding cages with five animals per cage. The severity of nasal symptoms, including itching, sneezing, and runny nose, was evaluated within 30 min following the final nasal sensitization[15]. Briefly, sneezing: (1 point for 1–3 consecutive sneezes, 2 points for 4–10 sneezes, 3 points for ≥ 11 sneezes); nasal itching: (1 point for lightly scratching the nose 1–2 times, 2 points for vigorously scratching around the nose and rubbing everywhere); runny nose: (1 point for discharge limited to the nostrils, 2 points for discharge exceeding the anterior nostril, 3 points for visible runny face). Rats with a total score exceeding 5 points indicated successful modeling.

Cytokine and OVA-specific IgE detection in nasal lavage fluid

In accordance with the literature[32], we collected nasal lavage fluid. After the final nasal OVA challenge, rats were anesthetized with pentobarbital (50 mg/kg), and an epidural anesthesia tube was then inserted 2 cm into the nasal cavity. The rats were placed in an inverted position, and both cavities were lavaged with 2 ml of phosphate-buffered saline (PBS) at a speed of 2 ml over 5 min. The collected NLF was centrifuged at 900 × g for 15 min, and the supernatant was stored at -80℃. The collected NLF were subjected to centrifugation at 900 xg for 15 min in 4 °C. The concentrations of inflammatory cytokines and OVA-specific IgE in the NLF were analyzed using ELISA kits for IL-4 (TAE-384r), IL-5 (TAE-662r), IL-6 (TAE-385r), IL-13 (TAE-373r), TNF-α (TAE-569r) and IL-1β (TAE-370r), OVA-specific IgE (TAE-348r) following the manufacturer's instructions. All measurements were conducted at an optical density (O.D) of 492 nm. The ELISA kits were obtained from Tianjin Anoric Biotechnology CO.ltd.

Histopathological evaluation of the nasal cavity and colon

After the last challenge, rats were euthanized by intravenous injection of sodium pentobarbital (100 ~ 150 mg/kg). Samples of nasal mucosa and colon tissues were immediately preserved in 4% paraformaldehyde. 48 h later, tissues were dehydrated and then embedded in paraffin for further processing and analysis. Thin Sect. (4 μm) were prepared for hematoxylin and eosin (H&E) staining. Additionally, sections of the nasal mucosa were stained with Toluidine Blue. Three high-power fields (HPF, × 400 and × 200) were captured per slice with an optical microscope (TC-C-TC, Nikon, Tokyo, Japan). Eosinophils and mast cell counts were performed for sections of the nasal mucosa and the mean values were calculated.

Assessment of blood lipids, LPS, inflammatory indicators and OVA-specific IgE in serum

Serum was isolated from blood samples, and the concentrations of total cholesterol (TC), triglycerides (TG), low-density lipoprotein cholesterol (LDL-C) and high-density lipoprotein cholesterol (HDL-C) were measured using enzymatic kits on an automated blood analyzer (Bayercorp). The TC (A111-1-1), TG (A110-1-1), LDL-C (A112-1-1) and HDL-C (A112-1-1) kits were supplied by NanJing Jiangcheng Bioengineering Institute. The serum levels of lipopolysaccharide (LPS), IL-4, IL-5, IL-6, IL-13, TNF-α, IL-1β and OVA-specific IgE were determined using ELISA kit at an optical density (O.D) of 492 nm. LPS (TAE-261r) kits, along with kits for the same inflammatory factors and OVA-specific IgE as those used in NLF, are supplied by Tianjin Anoric Biotechnology Co., Ltd.

Cell culture and treatment

THP-1 cells, a human monocytic cell line derived from an acute monocytic leukemia patient, and RPMI-1640 complete medium (including 0.05 mM β-mercaptoethanol, 1% penicillin/streptomycin, and 10% fetal bovine serum) were obtained from Procell Life Science & Technology Co., Ltd (Wuhan, China). The cells were identified by the STR genotype test. Experiments were conducted with the use of mycoplasma-free cells. The cells were incubated in a standard cell incubator with 5% CO2. THP-1 cells were seeded at a density of 1×10^6 cells per well in a 6-well plate and treated with 100 ng/mL phorbol 12-myristate 13-acetate (PMA, P8139; Sigma-Aldrich) for 24 h to induce macrophage differentiation. Differentiated macrophages were then pretreated with 26 μg/mL palmitic acid (PA) (P0500; Sigma) for 48 h, followed by stimulation with 100 ng/mL LPS (L2880; Sigma-Aldrich) and 20 ng/mL interferon gamma (IFN-γ, 300–02; PeproTech, Suzhou, China) for an additional 48 h in RPMI-1640 to induce inflammatory responses.

CCK-8 assay

THP-1 cells were seeded at 1×10^5 cells/well in a 96 well plates, and were treated with LPS + IFN-γ and different doses of palmitic acid (PA) (25 μM, 50 μM, 100 μM, 200 μM, 400 μM, and 800 μM). Cell viability was analyzed with a CCK-8 kit (HY-K0301; Med Chem Express, Newjersey, USA). The absorbance was determined at 452 nm using microplate reader (VICTOR Vivo, USA).

Oil red O staining

The macrophages differentiated from the THP-1 cell line were fixed in 4% paraformaldehyde solution (*v/v*) for 10 min and then washed with PBS for 30 s. Subsequently, the cells were stained with a filtered Oil Red O solution at room temperature for 20 min and rinsed in washing buffer for 30 s. After an additional wash with PBS for 20 s, images were acquired using an Olympus microscope (C-S-HS, Nikon, Tokyo, Japan).

Immunofluorescence and immunohistochemical evaluation

Immunofluorescence staining was performed as previous described[33], Briefly, 4 μm sections of nasal mucosa and colon tissues were prepared. Following deparaffinization, hydration, and antigen retrieval, the colon tissue sections were incubated overnight at 4℃ with primary antibodies against NLRP3 (1:200, YT5382), Caspase-1 (1:300, YT5743), NF-κB p65 (1:200, YP0191), all obtained from ImmunoWay Biotechnology Company (TX, USA). Subsequently, the sections were incubated with the corresponding secondary IgG antibodies. Nuclei were stained with DAPI for immunofluorescence (IF) analysis. Imaging was performed using a fluorescence microscope (TC-C-TC, Nikon, Tokyo, Japan).

Immunohistochemical staining was performed as follows. Nasal mucosal tissue and colon tissue sections were initially stained with H&E and then sealed. Then, the nasal mucosal tissue sections were incubated overnight at 4℃ with primary antibodies against NLRP3 (1:300, YT5382, ImmunoWay Biotechnology Company, TX, USA), NF-κB p65 (1:300, YP0191, ImmunoWay Biotechnology Company, TX, USA). The colon tissue sections were similarly incubated with primary antibodies against ZO-1(1:2000, 21773-1-AP, Proteintech, Wuhan, China) and Occludin (1:800, 13409-1-AP, Proteintech, Wuhan, China). Following overnight incubation, the sections were incubated with HRP-labelled secondary antibody. Color development was achieved using 3,3'-diaminobenzidine (DAB). The ratio of positively stained areas was quantified in three regions under a light microscope (C-S-HS, Nikon, Tokyo, Japan).

Western blot analysis

Proteins were extracted from the nasal mucosa tissue, colon tissue and THP-1 cells, and then lysed in RIPA buffer (R00100, Solarbio, Beijing, China) containing phosphatase and protease inhibitor mix (P1045, Beyotime, Shanghai, China). The total protein concentration was determined with the enhanced BCA kit (P0012, Beyotime, Shanghai, China). After gel electrophoresis, 30 μg of protein samples were transferred to PVDF membranes (Immobilon Merck KGaA, Darmstadt, Germany). Then, the membrane was blocked with 5% non-fat dry milk in TBST for 2 h at room temperature. Subsequently, the membrane were incubated overnight at 4℃ with the folllowing primary antibodies: anti-NLRP3 (1:1000, YT5382, ImmunoWay Biotechnology Company, TX, USA),

Primer	Sequences (5′–3′)
Rat NLRP3	Forward: 5′-GGTCCCGGTGACCTTGTGTG-3′
	Reverse: 5′-TGTCCTGAGCCATGGAAGCA-3′
Rat Caspase-1	Forward: 5′-AGGTGGCGCATTTCCTGGAC-3′
	Reverse: 5′-GGCAAGACGTGTACGAGTGGG-3′
Rat ASC	Forward: 5′-CAGTGCGGGAAGGCTATGGG-3′
	Reverse: 5′-CAGCCAGCTCCTGTATGCCC-3′
Rat NF-κB p65	Forward: 5′-TTAGCCAGCGCATCCAGACC-3′
	Reverse: 5′-TTGAGCTCGGCAGTGTTGGG-3′
Rat GAPDH	Forward: 5′-CAGCCGCATCTTCTTGTGC-3′
	Reverse: 5′-GGTAACCAGGCGTCCGATA-3′

Table 1. Primer sequences in animal experiment.

Primer	Sequences (5′–3′)
Homo NLRP3	Forward: 5′-GCCACGCTAATGATCGAC-3′
	Reverse: 5′-TCTGAACCCCACTTCGG-3′
Homo Caspase-1	Forward: 5′-CCACAATGGGTCCTGTTT-3′
	Reverse: 5′-GCATCTGCGCTCTACCA-3′
Homo NF-κB p65	Forward: 5′-GTGTTTGTCCAGCTTCG-3′
	Reverse: 5′-TCTGAACCCCACTTCGG-3′
Homo GAPDH	Forward: 5′-GGGGCTCTCCAGAACATC-3′
	Reverse: 5′-TGACACGTTGGCAGTGG-3′

Table 2. Primer sequences in cell experiment.

anti-Caspase-1 (1:1000, YT5743, ImmunoWay Biotechnology Company, TX, USA), anti-NF-κB p65 (1:1000, YP3108, ImmunoWay Biotechnology Company, TX, USA), anti-TMSI/ASC (1:1000, ab180799, Abcam), anti-p-NF-κB p65 (1:1000, YP0191, ImmunoWay Biotechnology Company, TX, USA), anti-Cleaved-Caspase-1 (1:2000, AF4022, Affinity Biosciences, Jiangsu, China) and anti-GAPDH (1:3000, YN5585, ImmunoWay Biotechnology Company, TX, USA). Following incubation, the membranes were washed and incubated with a suitable secondary antibody (1:5000, ZSGB-BIO Biosciences Ltd, Beijing, China) for 2 h at room temperature. Gel imaging was performed to detect the proteins, and ImageJ software (ImageJ Lnk 1.8.0, USA) was used for analysis.

Real-time PCR

Total RNA was extracted from cells and tissues using RNA isolation reagents (Trizol, G3013 Servicebio, Wuhan, China) following the manufacturer's instructions. Subsequently, 1 μg of total RNA was reversely transcribed into cDNA for PCR amplification using the PrimeScript™ RT reagent Kit with gDNA Eraser (RR047A, Takara, Tokyo, Japan). Quantitative real-time PCR was then performed using the TB Green® Premix Ex Taq™ II (RR820A, Takara, Tokyo, Japan) along with specific primers (Tables 1 and 2). GAPDH was employed as the internal control. The relative mRNA levels were determined as fold changes relative to the internal control and computed using the $2^{(-\Delta\Delta CT)}$ method.

Statistical analysis

Statistical analyses were conducted with GraphPad Prism 9 software (version 9.3.0, GraphPad Software, San Diego, CA, USA). One-way ANOVA was employed to assess the differences among multiple groups, while student's t-test was applied to assess significant differences between two specific groups. Data are presented as mean ± standard deviations (SD) from at least three independent experiments. $P < 0.05$ was considered statistically significant.

Data availability

The datasets in the study are available from corresponding author upon reasonable request.

Received: 8 October 2024; Accepted: 8 April 2025
Published online: 15 April 2025

References

1. Zhang, W., Ba, G., Tang, R., Li, M. & Lin, H. Ameliorative effect of selective NLRP3 inflammasome inhibitor MCC950 in an ovalbumin-induced allergic rhinitis murine model. *Int. Immunopharmacol.* **83**, 106394 (2020).

2. Cheng, L. et al. Chinese society of allergy guidelines for diagnosis and treatment of allergic rhinitis. *Allergy Asthma Immunol. Res.* **10**, 300–353 (2018).
3. Juvekar, M. R. et al. A Real-World observational study to evaluate the safety and effectiveness of fluticasone furoate-oxymetazoline fixed dose combination nasal spray in patients with allergic rhinitis. *Clin. Drug Investig.* **44**, 123–130 (2024).
4. Yuan, Y. et al. Obesity-Related Asthma: Immune Regulation and Potential Targeted Therapies. *J. Immunol. Res* 1943497 (2018).
5. Lim, J. J., Reginald, K., Say, Y. H., Liu, M. H. & Chew, F. T. A dietary pattern for high estimated total fat amount is associated with enhanced allergy sensitization and atopic diseases among Singapore/Malaysia young Chinese adults. *Int. Arch. Allergy Immunol.* **184**, 975–984 (2023).
6. Bolte, G. et al. Margarine consumption and allergy in children. *Am. J. Respir Crit. Care Med.* **163**, 277–279 (2001).
7. Lin, Y. P. et al. Associations between respiratory diseases and dietary patterns derived by factor analysis and reduced rank regression. *Ann. Nutr. Metab.* **68**, 306–314 (2016).
8. Yu, H. et al. Apigenin ameliorates non-eosinophilic inflammation, dysregulated immune homeostasis and mitochondria-mediated airway epithelial cell apoptosis in chronic obese asthma via the ROS-ASK1-MAPK pathway. *Phytomedicine* **111**, 154646 (2023).
9. Yang, Z. et al. Involucrasin B suppresses airway inflammation in obese asthma by inhibiting the TLR4-NF-κB-NLRP3 pathway. *Phytomedicine* **132**, 155850 (2024).
10. Jeong, J. S. et al. The absence of thioredoxin-interacting protein in alveolar cells exacerbates asthma during obesity. *Redox Biol.* **73**, 103193 (2024).
11. Hur, J., Kang, J. Y., Kim, Y. K., Lee, S. Y. & Lee, H. Y. Glucagon-like peptide 1 receptor (GLP-1R) agonist relieved asthmatic airway inflammation via suppression of NLRP3 inflammasome activation in obese asthma mice model. *Pulm Pharmacol. Ther.* **67**, 102003 (2021).
12. Bousquet, J. et al. Next-generation allergic rhinitis and its impact on asthma (ARIA) guidelines for allergic rhinitis based on grading of recommendations assessment, development and evaluation (GRADE) and real-world evidence. *J. Allergy Clin. Immunol.* **145**, 70–80 (2020).
13. Niimi, A. Redefining one airway, one disease: Broader classification considering specific pathophysiology and treatment. *Respir Investig.* **59**, 573–575 (2021).
14. Akhavanakbari, G. et al. Effect of high fat diet on NF-κB microRNA146a negative feedback loop in ovalbumin-sensitized rats. *Biofactors* **45**, 75–84 (2019).
15. Long, R. et al. Bencycloquidium bromide inhibits nasal hypersecretion in a rat model of allergic rhinitis. *Inflamm. Res.* **64**, 213–223 (2015).
16. Dudele, A. et al. Chronic exposure to low doses of lipopolysaccharide and high-fat feeding increases body mass without affecting glucose tolerance in female rats. *Physiol. Rep.* **3** (2015).
17. Mo, X. et al. Insoluble yeast β-glucan attenuates high-fat diet-induced obesity by regulating gut microbiota and its metabolites. *Carbohydr. Polym.* **281**, 119046 (2022).
18. Wang, Y. et al. Nuciferine modulates the gut microbiota and prevents obesity in high-fat diet-fed rats. *Exp. Mol. Med.* **52**, 1959–1975 (2020).
19. Rohr, M. W., Narasimhulu, C. A., Rudeski-Rohr, T. A. & Parthasarathy, S. Negative effects of a high-fat diet on intestinal permeability: A review. *Adv. Nutr.* **11**, 77–91 (2020).
20. Tuomi, K. & Logomarsino, J. V. Bacterial lipopolysaccharide lipopolysaccharide-binding protein, and other inflammatory markers in obesity and after bariatric surgery. *Metab. Syndr. Relat. Disord.* **14**, 279–288 (2016).
21. Isnard, S. et al. Gut leakage of Fungal-Related products: Turning up the heat for HIV infection. *Front. Immunol.* **12**, 656414 (2021).
22. Hara, S., Tojima, I., Shimizu, S., Kouzaki, H. & Shimizu, T. 17,18-Epoxyeicosatetraenoic acid inhibits TNF-α-induced inflammation in cultured human airway epithelium and LPS-Induced murine airway inflammation. *Am. J. Rhinol Allergy* **36**, 106–114 (2022).
23. Zhang, M., Liu, L. & Wang, S. Role of immune deviation by toll-liked receptor's doping LPS in pathogenesis of allergic rhinitis. *Zhonghua Er Bi Yan Hou Tou Jing Wai Ke Za Zhi* **49**, 288–293 (2014).
24. Ding, M., Wei, X., Liu, C. & Tan, X. Mahuang Fuzi Xixin decoction alleviates allergic rhinitis by inhibiting NLRP3/Caspase-1/GSDMD-N-mediated pyroptosis. *J. Ethnopharmacol.* **327**, 118041 (2024).
25. Bai, X. et al. Water-extracted *lonicera japonica* polysaccharide attenuates allergic rhinitis by regulating NLRP3-IL-17 signaling axis. *Carbohydr. Polym.* **297**, 120053 (2022).
26. Ma, M., Li, G., Qi, M., Jiang, W. & Zhou, R. Inhibition of the inflammasome activity of NLRP3 attenuates HDM-Induced allergic asthma. *Front. Immunol.* **12**, 718779 (2021).
27. Tolhurst, G. et al. Short-chain fatty acids stimulate glucagon-like peptide-1 secretion via the G-protein-coupled receptor FFAR2. *Diabetes* **61**, 364–371 (2012).
28. Zhou, H. et al. Activation of NLRP3 inflammasome contributes to the inflammatory response to allergic rhinitis via macrophage pyroptosis. *Int. Immunopharmacol.* **110**, 109012 (2022).
29. Everaere, L. et al. Innate lymphoid cells at the interface between obesity and asthma. *Immunology* **153**, 21–30 (2018).
30. Wen, H. et al. Fatty acid-induced NLRP3-ASC inflammasome activation interferes with insulin signaling. *Nat. Immunol.* **12**, 408–415 (2011).
31. D'Arqom, A., Luangwedchakarn, V., Umrod, P., Wongprompitak, P. & Tantibhedyangkul, W. Effects of 1α,25 dihydroxyvitamin D3 on pro-inflammatory cytokines of palmitic acid treated Thp-1 cells. *J. Food Sci.* **82**, 3013–3020 (2017).
32. Wang, W. & Zheng, M. Mucin 5 subtype AC expression and upregulation in the nasal mucosa of allergic rhinitis rats. *Otolaryngol. Head Neck Surg.* **147**, 1012–1019 (2012).
33. Wang, Z. et al. Panaxadiol inhibits programmed cell death-ligand 1 expression and tumour proliferation via hypoxia-inducible factor (HIF)-1α and STAT3 in human colon cancer cells. *Pharmacol. Res.* **155**, 104727 (2020).

Acknowledgements

The authors would like to express their gratitude to all the researchers involved in the study, as well as to the First Affiliated Hospital of Chongqing Medical University for providing the research platform.

Author contributions

S.P.P. was instrumental in concluding the experiment, composing the initial manuscript. X.Y.C. and J.T. conducted analyses and interpreted the results. X.F.Z. was involved in animal experimentation. X.Y.H. and J.X.H. were responsible for the collation of the data. J.L. made a significant contribution to the study in several key areas, including its conceptualization, supervision, the drafting and revision of the manuscript, and the acquisition of funding. The final manuscript has been reviewed and approved by all the authors. All the authors agreed the consent for publication.

Funding
This work was supported by the First Affiliated Hospital of Chongqing Medical University (No. 03010203XKTS065).

Declarations

Competing interests
The authors declare no competing interests.

Ethical approval
The study was approved by the Animal Experiment Ethics Committee of Chongqing Medical University (Approval number: IACUC-CQMU-2024-0436).

Additional information
Supplementary Information The online version contains supplementary material available at https://doi.org/10.1038/s41598-025-97978-1.

Correspondence and requests for materials should be addressed to J.L.

Reprints and permissions information is available at www.nature.com/reprints.

Publisher's note Springer Nature remains neutral with regard to jurisdictional claims in published maps and institutional affiliations.